Transition-State Analysis of Nucleoside Hydrolase from *Crithidia fasciculata*†

Benjamin A. Horenstein, David W. Parkin,‡ Bernardo Estupiñán, and Vern L. Schramm*

Department of Biochemistry, Albert Einstein College of Medicine, 1300 Morris Park Avenue, Bronx, New York 10461

Received June 19, 1991; Revised Manuscript Received August 15, 1991

ABSTRACT: The transition state of nucleoside hydrolase from the trypanosome *Crithidia fasciculata* has been characterized by multiple V_{max}/K_m kinetic isotope effects with labeled inosine and adenosine as substrates. Nucleoside hydrolase catalyzes the hydrolysis of the N-glycosidic linkage of the commonly occurring purine and pyrimidine nucleosides, with V_{max}/K_m ranging over 2 orders of magnitude. The kinetic isotope effects for inosine were [1′-^{3}H] = 1.150 ± 0.006, [2′-^{3}H] = 1.161 ± 0.003, [1′-^{14}C] = 1.044 ± 0.004, [9-^{15}N] = 1.026 ± 0.004, [4′-^{3}H] = 0.992 ± 0.003, and [5′-^{3}H] = 1.051 ± 0.003. The magnitude of the kinetic isotope effects for inosine, an equivalent [1′-^{3}H] kinetic isotope effect for the poor substrate adenosine, and the rapid equilibrium random kinetic mechanism [Parkin D, W., Horenstein, B. A., Abdulah, D. R., Estupiñán, B., & Schramm, V. L. (1991) *J. Biol. Chem.* (in press)] all indicate that the isotope effects are fully expressed. The kinetic and solvent deuterium isotope effects have been used to analyze the transition-state structure using bond energy bond order vibrational analysis. The transition state involves a protonated hypoxanthine leaving group with a C–N glycosidic bond elongated to approximately 2 Å. The ribose group contains substantial carbocationic character, unusually strong hyperconjugation of H2′, and a bond length of approximately 3 Å to the incoming oxygen nucleophile. The remote isotope effect (4′-^{3}H and 5′-^{3}H) and the results of transition-state calculations provide the most detailed description of the steric and bonding properties of an enzyme-stabilized transition state.

Nucleoside hydrolase from the trypanosome *Crithidia fasciculata* catalyzes the hydrolysis of purine and pyrimidine ribonucleosides to the constituent base and ribose (Parkin et al., 1991a):

$$\text{nucleoside} + H_2O \rightleftarrows \text{ribose} + \text{base}$$

The kinetic mechanism is rapid-equilibrium random with respect to product release (Parkin et al., 1991a). The pH profiles of kinetic constants reveal no ionic interactions for substrate binding but identify two anions with pK_a values near 6.1 which are essential for catalysis. These findings suggest that two carboxylates stabilize an oxocarbonium-like transition state. Previous work from this laboratory (Mentch et al., 1987; Parkin et al., 1991b) has established transition-state structures for two different AMP nucleosidases, both of which are oxocarbonium ion in character. Studies on inosine hydrolase extend these findings to an enzyme which is involved in purine nucleoside salvage in trypanosomes. In addition, the results provide information on common and unique features of the transition states of nucleoside and nucleotide N-glycohydrolases. The transition state mediated by nucleoside hydrolase has been characterized using multiple kinetic isotope effects and bond energy bond order vibrational analysis (BEBOVIB). A detailed description of the nucleoside hydrolase transition state is reported. Several remote kinetic isotope effects, not previously observed for enzymatic catalysis, provide additional information about the structure and geometry of the transition state.

Materials and Methods

Nucleoside Hydrolase. Nucleoside hydrolase was purified from *C. fasciculata* as described by Parkin et al. (1991a). All enzyme used was >95% homogeneous by denaturing gel electrophoresis.

Isotopically Labeled Inosine and Adenosine. Isotopically labeled AMP's were prepared enzymatically from appropriately labeled glucose, ribose, and adenine (Parkin & Schramm, 1987). Radiolabeled inosine and adenosine were prepared enzymatically from the corresponding AMP. Labeled adenosine nucleosides were prepared by treatment of the corresponding AMP with 1–2 units of calf intestine alkaline phosphatase (P-L Biochemicals) in 100 mM triethanolamine, pH 8.0 at 37 °C, in the presence of 12 nM (*R*)-deoxycoformycin to inhibit adenosine deaminase activity. Labeled inosines were prepared by treatment of the corresponding adenosines with 3 units of adenosine deaminase (Sigma) in 100 mM triethanolamine, pH 8.0/1.5 mM $MgCl_2$, 37 °C. The reactions were monitored by reverse-phase HPLC and quenched when complete by heating at 100 °C for 4 min. The nucleosides were purified by reverse-phase HPLC on a Waters Bondapack C_{18} column at 2.0 mL/min flow rate with detection at 257 nm. Adenosine was eluted with 9.9 mM ammonium acetate, pH 5, in 1% MeOH. Inosine was purified in 9.5 mM ammonium acetate, pH 5, in 5% MeOH. Fractions containing the desired nucleoside were pooled, concentrated, and diluted to approximately 3 μCi/mL in 50% aqueous ethanol and stored at −70 °C. The isotopically labeled compounds prepared for this study are listed in Table I.

Measurement of Kinetic Isotope Effects. Kinetic isotope effects were determined by measurement of the relative rates of hydrolysis of nucleoside containing a heavy or light (natural abundance) isotope in a given position. The substrate contained an isotopic mixture of both ^{3}H and ^{14}C species in the ribosyl residue. One radiolabel was located in the isotopically sensitive position (the heavy substitution) while the light substitution was marked by incorporation of the other radio-

† Primary support was provided by Research Grant GM41916 from the National Institutes of Health. Preliminary work was supported by Research Grant GM21083 from the National Institutes of Health. Postdoctoral support for B.A.H. was also by Grant PF-3298 from the American Cancer Society and a Mildred and Emil Holland Postdoctoral Scholarship from the Albert Einstein College of Medicine.

* To whom correspondence should be addressed.

‡ Current address: Department of Chemistry, Chestnut Hill College, Germantown Ave., Philadelphia, PA 19118.

0006-2960/91/0430-10788$02.50/0

label in the 5′-position of the ribosyl residue, remote from the reaction center. The [1′-^{14}C]- and [9-^{15}N]inosine kinetic isotope effects relied on [5′-^{3}H]inosine to report on the light isotope. However, a significant kinetic isotope effect was determined for [5′-^{3}H]inosine, so it was necessary to correct the [1′-^{14}C] and [9-^{15}N] kinetic isotope effects by the value of the [5′-^{3}H] kinetic isotope effect. For each kinetic isotope effect experiment, two reactions were run, one to 20–30% completion and the other to 100% completion. The 100% reaction provides the control ratio of ^{3}H/^{14}C and the 20–30% reaction provides the ^{3}H/^{14}C ratio changed by the presence of a kinetic isotope effect. The ^{3}H/^{14}C ratio in the product ribose was measured as previously described (Parkin et al., 1984) in order to calculate the kinetic isotope effect. As this is a trace-label technique, the information obtained from these experiments is V_{max}/K_m kinetic isotope effects.

Calculation of Kinetic Isotope Effects. Kinetic isotope effects were measured by analyzing multiple samples removed from an isotope-effect reaction mixture containing ^{14}C- and ^{3}H-labeled substrates. Samples were analyzed in triplicate or quadruplicate as indicated in Table I. The ^{3}H/^{14}C ratio was measured by scintillation counting of the product ribose following fractionation of ribose on a charcoal/cellulose column. Each cycle of the scintillation counter allowed calculation of ^{3}H/^{14}C ratios for each sample. The average ^{3}H/^{14}C ratios for partial and complete conversion to products were calculated and then expressed as the ratio to provide the observed kinetic isotope effect for one cycle. At least six cycles of scintillation counter analysis were used to calculate the average kinetic isotope effect for all cycles. The standard deviation of the average was calculated from the results of all cycles, from all samples.

Solvent Deuterium Isotope Effect. Triethanolamine buffers, 50 mM, pH/pD 7.5 in H_2O/D_2O (99.9% D, Aldrich), were used for this experiment. Inosine was employed as substrate; initial velocity measurements were made at 30 °C measured spectrophotometrically at 280 nm, on the basis of the differential absorption of inosine and the product hypoxanthine. Differential extinction coefficients for hypoxanthine/inosine in the H_2O and D_2O solutions were determined and found to be equal, with a decrease of 0.94 OD/μmol of hypoxanthine formed. The data were fitted to the equation

$$v = VA/(K(1 + IVK_I) + A(1 + IV_I))$$

where v initial reaction rate, $V = V_{max}$, A = inosine concentration, $K = K_m$, I = fractional substitution with D_2O, V_I = V isotope effect −1 and $VK_I = V_{max}/K_m$ isotope effect −1 using the routines of Cleland (1977).

Transition-State Modeling. The BEBOVIB-IV program (Quantum Chemistry Program Exchange, No. 337 (Sims et al., 1977), was used to model transition-state geometries which would provide kinetic isotope effects to match the experimentally determined values. Acceptable transition states were chemically reasonable structures which produced calculated isotope effects which simultaneously satisified all of the experimentally determined isotope effects at positions C1′, H1′, H2′, H4′, H5′, and N9. The atoms of reactant-state inosine are given in Figure 1, together with bond lengths and geometry.

Bond lengths and angles for the reactant inosine were taken from the crystal structure (Munns & Tollin, 1970). Bond lengths for C–H bonds were obtained by AMPAC calculations.[1] Force constants for the various vibrational modes were derived from reported values (Sims & Lewis, 1984; Sims & Fry, 1974; Wilson et al., 1955). Due to limitations on the maximum number of atoms employed in a BEBOVIB model, only the relevant atoms for the transition-state structure were used. The validity of using a truncated atomic structure is discussed by Sims and Lewis (1984). The reactant-state structure for the truncated inosine included ribosyl and imidazole ring moieties but omitted the 3′-hydroxyl group and the other hydroxylic hydrogen atoms.

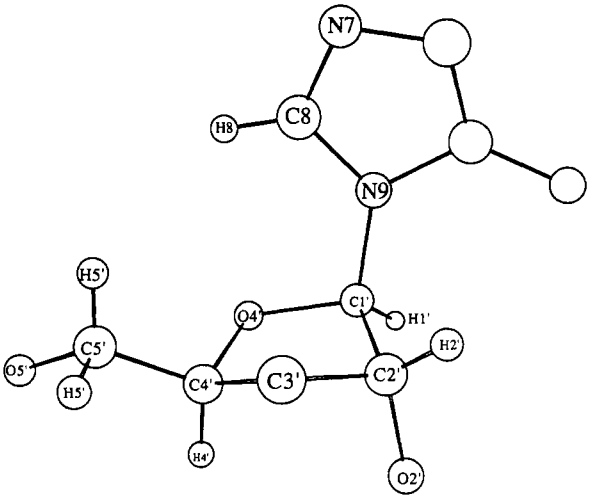

Key Reactant State Bond Lengths

Bond	Length, Å	Bond	Length, Å
C1′-N9	1.477	C2′-H2′	1.128
C1′-O4′	1.417	N9-C8	1.372
C1′-C2′	1.530	C8-N7	1.308
C1′-H1′	1.128		

FIGURE 1: Structure, nomenclature, and bond lengths of the reactant inosine used in BEBOVIB calculations. Coordinates of Munns and Tollin (1970) were used to construct the model. Bond lengths for carbon–hydrogen bonds are from AMPAC calculations.

The starting structure for the transition state of the ribose ring portion of inosine was derived from the X-ray crystal structure coordinates for ribonolactone (Kinoshita et al., 1981). The starting C–H bond lengths were set equal to the values used for the ribose portion of inosine. The incoming oxygen nucleophile (O′ in Figure 1) was modeled as an O atom, placed 180° with respect to the breaking C1–N9 glycosidic bond. Both the forming and breaking bonds were placed orthogonal to the plane defined by the atoms attached to C1′. The calculations are insensitive to wheter O or H_2O is used as the attacking nucleophile. AMPAC calculations were employed to estimate the bond order changes that occur in the hypoxanthine residue of inosine in proceeding to the N7–H tautomer of hypoxanthine at the transition state. The calculations were performed on 9-methylhypoxanthine and N7–H hypoxanthine. Significant changes in bond order were predicted between the bonds N9–C8–N7, while insignificant changes were observed elsewhere in the hypoxanthine ring. The sum of the bond order in the N9–C8–N7 bonds was conserved in both structures. The bond order ratio, defined as $N7\text{–}C8_{BO}/C8\text{–}N9_{BO}$ varied from 1.246 to 0.873 for the reactant and product states, respectively. This information was used to relate glycosidic C1′–N9 bond order to the bond order in the N9–C8 and C8–N7 bonds. For the reactant-state structure of inosine, where $x = C8\text{–}N9_{BO}$ and $1.246x = N7\text{–}C8_{BO}$, the sum of the bonds equals $1.246x + x = 3.34$, so $x = 3.34/2.246$. Likewise, for the product structure of hypoxanthine, where $x = C8\text{–}N9_{BO}$ and $0.873x = N7\text{–}C8_{Bo}$, the sum of the bonds equals $0.873x + x = 3.34$, so $x = 3.34/1.873$. In going from reactant to

[1] AMPAC (Quantum Chemistry Program Exchange. No. 506) calculations employed the AM1 parameter set (Dewar et al., 1985).

product, the denominator decreases by 0.373, and this amount is adjusted by the fraction of glycosidic bond cleavage = (1.051 − (C1′–$N9_{BO\text{-}TS}$))/1.051, where 1.051 = C1′–$N9_{BO}$ for the reactant inosine, taken from the crystal structure, and C1′–$N9_{BO\text{-}TS}$ is the bond order in the transition state. The bond order in the C8–N7 bond will always equal 3.34 − (C8–$N9_{BO}$), thus eqs 1 and 2 will predict the redistribution of bonds in

$$C8\text{–}N9_{BO} = 3.34/(2.246 - (((1.051 - (C1'\text{–}N9_{BO}))/1.051)0.373)) \quad (1)$$

$$N7\text{–}C8_{BO} = 3.34 - (C8\text{–}N9_{BO}) \quad (2)$$

N7–C8–N9 of the departing hypoxanthine as the N-glycosidic bond is broken. Thus, the N7–C8 and C8–N9 bonds were varied between limiting values as a function of the fraction of cleavage of the glycosidic linkage.

The reaction coordinate was generated by coupling the stretching motion of the breaking C1′–N9 bond with the forming C1′–O′ bond from the attacking oxygen. Walden inversion was incorporated into the model by introducing a weak interaction force constant of ±0.05 between the stretching modes O′–C1′ and C1′–N9 with the angle bending modes defined by O′–C1′–H1′, O′–C1′–C2′, O′–C1′–O4′, N9–C1′–H1′, N9–C1′–C2′, and N9–C1′–O4′ (Markham et al., 1987). Reaction coordinates that were generated by simple translational separation by hypoxanthine from ribose (S_N1-like) produced no transition states compatible with the experimental data. Transition-state space was searched by varying bond orders to atoms for which isotope effects were measured. Families of structures were obtained which were consistent with the observed kinetic isotope effects. Additional details have been discussed in previous publications (Mentch et al., 1987; Parkin et al., 1991b).

Results

Kinetic Isotope Effect Experiments. The kinetic isotope effects obtained with nucleoside hydrolase are summarized in Table I. The large values observed for the secondary 1′-^{3}H and 2′-^{3}H kinetic isotope effects are indicative of a transition-state having substantial oxocarbonium ion character with sp^2-like hybridization at C1′ and expanded bonding between N9, C1′, and O′. Strong hyperconjugative interaction of H2′ with C1′ is necessary for the isotope effect observed with 2′-^{3}H. The maximum 1′-^{3}H kinetic isotope effect calculated for an S_N1 transition state with bond order approaching zero to the leaving group is approximately 1.5. The acid-catalyzed hydrolysis of inosine (Parkin & Schramm, 1984) gives a 1′-^{3}H kinetic isotope effect of 1.20, a value which is likely to be the practical upper limit for the isotope effect at that position. Pure carbocations are unstable reactive intermediates and should closely resemble their transition states according to the Hammond postulate (Hammond, 1955). However, the participation of solvent and/or active site residues in the enzyme-stabilized transition state prevents formation of a fully developed carbocation. The intermediate values for the 1′-^{14}C and 9-^{15}N kinetic isotope effects indicate that the bond between C1′ and N9 is not completely cleaved in the transition state.

The remote kinetic isotope effect of 1.05 from the 5′-^{3}H was much larger than previously observed for AMP nucleosidase, for a mutant form of the enzyme, or for acid-catalyzed solvolysis, all of which had values near unity (Parkin et al., 1984, 1991b; Parkin & Schramm, 1987). The size of this isotope effect indicates a major change in the environment of the 5′ hydrogen at the transition state. An isotope effect for the 4′ hydrogen of the ribosyl portion has not been previously reported for enzymatic or chemical hydrolysis of a nucleoside. The inverse nature of 0.992 for this kinetic isotope effect rules out any interaction which weakens the C4′–H4′ bond or which provides addition vibrational freedom for the 4′ hydrogen. Significant remote isotope effects at the 4′- and 5′-positions of inosine indicate that the enzyme-stabilized transition state contains distortions of the entire ribose ring beyond those which occur during acid-catalyzed solvolysis.

Table I: Kinetic Isotope Effects for Nucleoside Hydrolase

substrates	isotope and type of effect[a]	exptl kinetic isotope effect[b]
[1′-^{3}H]inosine + [5′-^{14}C]inosine	1′-^{3}H, α-secondary	1.150 ± 0.006 (3)
[2′-^{3}H]inosine + [5′-^{14}C]inosine	2′-^{3}H, β-secondary	1.161 ± 0.003 (4)
[1′-^{14}C]inosine + [5′-^{3}H]inosine	1′-^{14}C, primary	1.044 ± 0.004[c] (3)
[9,5′-^{15}N,^{14}C]inosine + [5′-^{3}H]inosine	9-^{15}N, primary	1.026 ± 0.004[c] (4)
[5′-^{3}H]inosine + [5′-^{14}C]inosine	5′-^{3}H, δ-secondary	1.051 ± 0.003 (4)
[4′-^{3}H]inosine + [5′-^{14}C]inosine	4′-^{3}H, γ-secondary	0.992 ± 0.003 (4)
[1′-^{3}H]adenosine + [5′-^{14}C]adenosine	1′-^{3}H, α-secondary	1.157 ± 0.003 (3)

[a] A primary isotope effect indicates that the isotope is a bonding atom in the breaking bond. Secondary isotope effects indicate that the isotope is one (α), two (β), three (γ), or four (δ) bonds distant from the breaking bond. [b] The number in parentheses is the number of experimental kinetic isotope effect measurements made for a kinetic isotope effect experiment. [c] The kinetic isotope effects obtained with [5′-^{3}H]-inosine as the reporter for the normal isotopic reaction rate were corrected for the 1.051 ± 0.003 isotope effect of the 5′-^{3}H. In cases where [5′-^{3}H]inosine was used as the remote label, the experimental isotope effect was corrected by the expression (observed isotope effect × 5′-^{3}H isotope effect).

Solvent Deuterium Isotope Effect. The solvent deuterium isotope effect on V_{max} was found to be 1.30 ± 0.07, and for V_{max}/K_m, 0.99 ± 0.07. The observation of a solvent kinetic isotope effect indicates a small contribution from proton transfer in the step(s) which occur following binding of the substrate. The value of unity for the V_{max}/K_m isotope effect indicates that the proton transfer step(s) provide no observable isotope effect between free enzyme and substrate and the first irreversible step in the reaction sequence. For nucleoside hydrolase reacting under initial rate conditions, cleavage of the glycosidic bond must be considered the first irreversible step. Proton transfer is thus not a major part of the transition state, with the proton transfer(s) having been completed prior to transition-state formation.

Transition-State Modeling. The process of converging on a transition-state structure which was consistent with the experimental isotope effects was simplified by the observation that the calculated 2′-^{3}H isotope effect was only sensitive to variations in the C2′–H2′ bond order when the dihedral angle between C2′–H2′ and C1′–N9 is nearly eclipsed. The ribonolactone model of the transition state predicts that C2′–H2′ would be nearly eclipsed with the C1′–N9 bond of the departing purine. All other isotope effects were independent of these variations. Figure 2 shows the calculated 2′-^{3}H isotope effect as a function of C2′–H2′ bond order and the experimental value. A bond order of 0.819 ± 0.001 was found to agree with the experimental value. The uncertainty in the bond order reflects the standard error of 0.003 associated with the experimental measurement of the kinetic isotope effect. All subsequent calculations on transition states included this C2′–H2′ bond order and the associated increase in bond order between C1′–C2′ due to the hyperconjugative interaction.

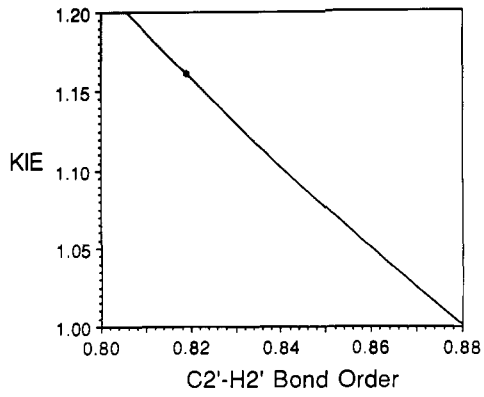

FIGURE 2: Effect of altered C2′–H2′ bond order on the β-secondary ^{3}H kinetic isotope effect. The ordinate gives the kinetic isotope effect for 2′-^{3}H as the C2′–H2′ bond order increases. The solid line is *calculated* 2′-^{3}H kinetic isotope effects from BEBOVIB-IV calculations. The *experimental* value, together with its standard error bars, was aligned with the calculated isotope effect. Note that even a small change in the placement of the experimental isotope effect causes disagreement with the calculated isotope effect. The dihedral angle between C2′–H2′ and C1′–N9 was set at 12° for this calculation.

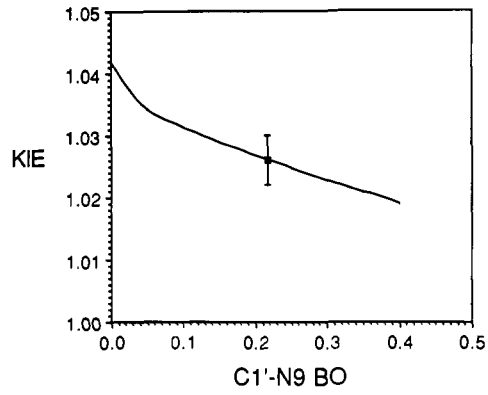

FIGURE 3: Effect of altered C1′–N9 bond order on the ^{15}N kinetic isotope at N9. The solid line is the ^{15}N kinetic isotope effect for N9 calculated with the BEBOVIB-IV routine as a function of the C1′–N9 bond order. The experimental point and associated standard errors indicate the C1′–N9 bond order which is consistent with the experimental data. The N7–C8 and C8–N9 bond orders were assigned according to eqs 1 and 2 as the C1′–N9 bond order was varied (see the Materials and Methods section).

The 9-^{15}N kinetic isotope effect is a function of the bond order between C1′–N9 and the electron distribution between the N9–C8 and C8–N7 bonds of the hypoxanthine residue (Figure 1). The relationship between the bond order of the breaking C1′–N9 bond, the calculated 9–^{15}N kinetic isotope effect, and the experimentally determined value are illustrated in Figure 3. A 9-^{15}N kinetic isotope effect of 1.026 ± 0.004 requires a C1′–N9 bond order of 0.22 ± 0.1. The uncertainty of the C1′–N9 bond order is based on the error in the experimental measurement and is illustrated in Figure 3. The magnitude of the 9-^{15}N isotope effect rules out transition states with C1′–N9 bonds below 0.12 bond order.

Kinetic isotope effects were also calculated for transition-state families in which the C1′–O4′ bond order of the oxocarbonium intermediate was fixed and the C1′–N9 and C1′–O′ bond orders were varied in order to match the 1′-^{14}C and 1′-^{3}H kinetic isotope effects. Figure 4 shows an example of this approach. Any C1′–N9 and C1′–O′ bond orders which did not simultaneously match the experimental kinetic isotope effects were eliminated. This approach established a transition-state structure having a C1′–N9 bond order of 0.225 ± 0.095 and is consistent with the data obtained from the 9-^{15}N isotope effect. The partial bond to the leaving group in the

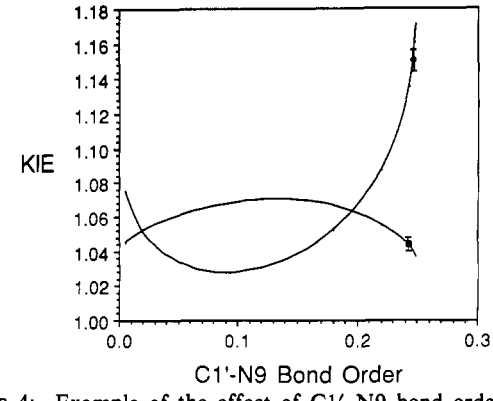

FIGURE 4: Example of the effect of C1′–N9 bond order on the calculated 1′-^{3}H and 1′-^{14}C kinetic isotope effects. The solid curves are the calculated isotope effects while the experimental 1′-^{3}H and 1′-^{14}C kinetic isotope effects are shown as the data points together with the associated experimental error. The concave-up curve is for the 1′-^{3}H isotope effect and the concave-down curve is for the 1′-^{14}C isotope effect. The C1′–N9 bond order consistant with the experimental data is 0.248. In this example, the sum of C1′–N9 + C1′–O bond orders was fixed at 0.250; the C1′–O4′ bond order was fixed at 1.62. Using the above approach, a family of transition states which satisfied the experimental data was identified in which the C1′–O4 bond order was 1.65 ± 0.25 and the sum of C1′–N9 + C1′–O′ bond order was 0.225 ● 0.095.

transition state indicated that the geometry at C1′ would not be completely rehybridized to sp^2 as expected for a pure S_N1 reaction. Equation 3 was used to describe the extent of rehybridization in the transition state

$$\alpha = 90° + 19.5° \text{ (C1′–N9 bonding)} \qquad (3)$$

where α is the angle described by N9, C1′, and any one of the three atoms attached to C1′ and C1′–N9 bonding is defined as (C1′–N9 bond order in the transition state)/(C1′–N9 bond order in the reactant state).

The geometry of C1′ was adjusted for partial bond formation between C1′–N9 in the transition state using eq 3 and the new structure analyzed by BEBOVIB calculations to determine the effect of the hybridization geometry on the calculated kinetic isotope effects. Only the 1′-^{3}H kinetic isotope effect was sensitive to change in α. Small changes in bond order between O′ and C1′ were then sufficient to produce agreement with the experimentally determined isotope effects.

The transition-state structure which is consistent with the experimental kinetic isotope effects is shown in Figure 5. The error limits on each of the bonds relates to the uncertainty in the experimental measurement of the kinetic isotope effects summarized in Table I. The transition state has substantial oxocarbonium ion character with the C1′–N9 glycosidic linkage nearly broken while the attacking oxygen nucleophile has very low bond development. The transition-state bond length between O4′ and C1′ is decreased substantially from 1.417 to 1.30 ± 0.05 Å, reflecting the oxocarbonium ion character of the transition state. The bond length at H2′ was increased from 1.128 to 1.160 Å to reflect the hyperconjugative interaction with C1′ as described above.

Discussion

Expression of Intrinsic Isotope Effects. The intrinsic nature of the isotope effects has been demonstrated by a combination of steady-state kinetic properties and the magnitude of the isotope effects. A rapid-equilibrium random mechanism for substrate addition and product dissociation has been established (Parkin et al., 1991a). This mechanism reveals that dissociation of products and substrate from the enzyme is much faster than conversion of inosine to products. This can only occur with a low commitment to catalysis and is consistent

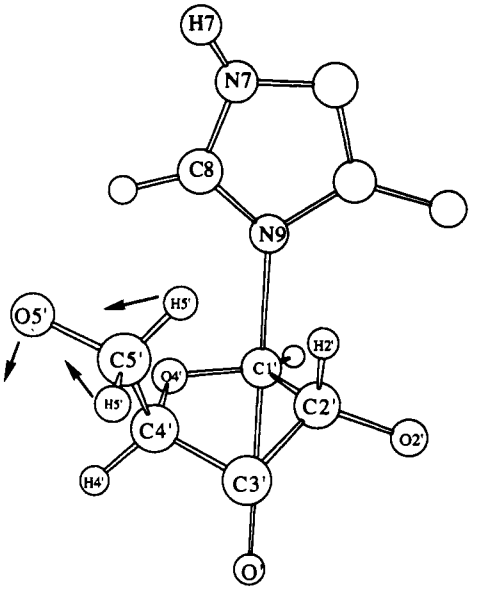

Transition State Bond Lengths

BOND	Bond Length
C1'-N9	1.97 ± 0.14 Å
C1'-O'	3.0 ± 0.4 Å
O4'-C1'	1.30 ± 0.05 Å
C2'-H2'	1.160 ± 0.001 Å
C1'-C2'	1.502 ± 0.001 Å
N7-C8	1.346 ± 0.006 Å
C8-N9	1.332 ± 0.006 Å

FIGURE 5: The transition state for nucleoside hydrolase. This structure gave a unique agreement with the family of kinetic isotope effects in Table I. The major features include protonation of the leaving group at N7, shift of the excess bond order from N7–C8 in the reactant state to C8–N9 in the transition state, the C1′–N9 glycosidic bond order substantially decreased, but large compared to the O′, the attacking oxygen nucleophile, and substantial rehybridization at C1′ toward sp^2. Note the large O4′–C1′ bond order compared to the reactant in Figure 1. The configuration of the ribose ring changes from 3′-endo to 3′-exo as C1′ rehybridizes. Modest distortion of the sp^3 configuration around C5′ causes the observed normal kinetic isotope effect. Arrows depict displacement of atoms which move as indicated to flatten the hydroxymethyl group in the transition state.

with the observation of intrinsic kinetic isotope effects. The V_{max}/K_m value for inosine is 7.6×10^{-4} M^{-1} s^{-1}, well below the level of 10^8–10^9 expected if every enzyme–inosine interaction resulted in product formation (Hammes & Schimmel, 1970; Fersht, 1977). The 1′- and 2′-^{3}H kinetic isotope effects are similar in magnitude to those found for the acid-catalyzed reaction (Parkin & Schramm, 1984). The presence of a significant commitment to catalysis would result in lower values for these isotope effects. The kinetic isotope effect for [1′-^{3}H]adenosine was measured under the same conditions and gave the same value as for the [1′-^{3}H]inosine experiment. Since V_{max}/K_m for inosine is 7.8 times greater than that for adenosine (Parkin et al., 1991a), any significant commitment would be expected to result in a lowered experimental kinetic isotope effect with inosine as the substrate. When intrinsic or near-intrinsic isotope effects are observed, the results provide direct information on the nature of the transition state.

Qualitative Transition-State Analysis. The isotope effects indicated that nucleoside hydrolase stabilizes an S_N1-like transition state which contains substantial oxocarbonium ion character. Strong hyperconjugative interactions are implicated by the magnitude of the β-secondary isotope effect. The α-secondary isotope effect predicts a ribosyl oxocarbonium ion with near sp^2 hybridization at C1′. Ribonolactone was used as the model compound for the transition-state analysis, on the basis of its known structure and its planarity at C1′. The bond order at H1′ of the transition-state structure for nucleoside hydrolase was increased slightly by 3.4% in order to reflect the sp^2 hybridization at C1′. The structural model for the departing hypoxanthine was an imidazole residue which was protonated at the N distal from the glycosidic linkage (equivalent to N7 of inosine). Without protonation, hypoxanthine would be a poor anionic leaving group. The acid-catalyzed solvolysis of inosine has been proposed to proceed largely through a monoprotonated hypoxanthine cation (Romero et al., 1978). The small solvent deuterium kinetic isotope effect of 1.30 indicates nearly complete transfer of at least one proton in the transition state. A proton in flight at the transition state, midway between donor and the N7 of hypoxanthine, would be expected to give an isotope effect near 6. Additional evidence for N7 protonation comes from the lack of substrate activity of tubercidin (7-deazadenosine), which lacks N7 (Parkin et al., 1991a). Finally, the value of the observed ^{15}N kinetic isotope effect requires bond orders to N9 that can only be rationalized in the presence of protonation at N7. The combination of these features provided the qualitative features for the transition-state structure. Quantitative analysis of the transition state used these features as starting points and refined the structure to match the kinetic isotope effects predicted by BEBOVIB-IV.

Reaction Coordinate Generation. S_N1 reaction coordinates which involved dissociation of the C1′–N9 bond without participation of the O′ nucleophile (Figure 5) gave calculated 9-^{15}N isotope effects which were greater than the experimental value. Similar results were obtained when the attacking O′ was included in the vibrational model but was not coupled to C1′–N9 vibration. Only reaction coordinates which involved coupling of C1′–O′ motion with C1′–N9 motion provided calculated isotope effects which agreed with the experimental values.

Kinetic Isotope Effects from 1′- and 2′-^{3}H. The 1′-^{3}H kinetic isotope effect of 1.150 is approaching the value of 1.23 observed for the acid-catalyzed hydrolysis of inosine (Parkin & Schramm, 1984). The unusually large value of 1.161 for the 2′-^{3}H kinetic isotope effect is diagnostic for the presence of hyperconjugation to C2′ in the transition state and simultaneously rules out an S_N2 displacement at C1′. The 2′-^{2}H kinetic isotope effect for the acid-catalyzed hydrolysis of adenosine 5′-monophosphate is 1.077 (Parkin & Schramm, 1984), and use of the Swain–Schaad relationship (Swain et al., 1958) predicts a ^{3}H kinetic isotope effect of 1.113. Since the β-secondary isotope effect seen for the nucleoside hydrolase reaction is larger than that found for chemical solvolysis, it is apparent that H2′ undergoes interactions on the enzyme which do not occur in solution. An explanation for the magnitude of the kinetic isotope effect is a ribosyl conformation in the active site which fixes the dihedral angle described by H2′–C2′ and C1′–N9 at or near 0°. This interaction maximizes hyperconjugative interaction (Sunko et al., 1977). In solution, this conformation could be one in a population of reactive conformations, some of which would not give rise to the maximum β-secondary kinetic isotope effect. On the enzyme, specific interaction of an active site residue(s) such as a carboxylate with the oxocarbonium ion could position the transition state at a location on the reaction coordinate which undergoes more hyperconjugation than in solution. Finally, hydrogen bonding to the 2′OH could stabilize the oxocarbonium ion through inductive effects (Johnson et al., 1988). The increase in electron density would result in a lengthening

of the C2′–H2′ bond, contributing to the observed isotope effect due to greater vibrational freedom of H2′. Interaction of enzymatic groups with the 2′-hydroxyl is also indicated by the substrate specificity of nucleoside hydrolase, where 2′-deoxynucleosides are poor or inactive as substrates (Parkin et al., 1991a). The attacking water can have only very low bond formation to C1′. Any O′–C1′ bond order above 0.019 caused the calculated 1′-^{3}H isotope effect to disagree with the experimental results. In the transition state, water is poised to trap the oxocarbonium ion but has little involvement in the cleavage of the glycosidic bond. It is unclear whether water or hydroxide is the attacking species since O′–C1′ bond formation is so weak at the transition state. At some point in the reaction coordinate, it is necessary for the attack to be completed by the hydroxyl as O′–C1′ bond formation occurs.

The attacking oxygen nucleophile is a specific water-derived ligand which has been activated by the enzyme. Attack of a general solvent nucleophile on an enzyme-stabilized oxocarbonium has been ruled out by demonstrating that methanol cannot attack the oxocarbonium to yield 1-methylriboside as product (Parkin et al., 1991a). Enzymes which permit attack on oxocarbonium-like intermediates readily form the products expected by methanol attack (Schuber et al., 1976).

Kinetic Isotope Effects from 1′-^{14}C. The primary 1′-^{14}C isotope effect is in the range expected for an S_N1-like transition state (Mentch et al., 1987). Its occurrence is an indication of less restricted motion at C1′ in the transition state relative to the ground state, consistent with an S_N1-like or highly expanded S_N2-like process. A symmetric S_N2 transition state around C1′ would cause a primary 1′-^{14}C isotope effect around 1.10 (Markham et al., 1987), considerably outside the observed range.

Kinetic Isotope Effects from 9-^{15}N. Loss of a full bond to N9 in the transition state predicts an isotope effect near 1.04. The intermediate value of 1.026 observed for the 9-^{15}N kinetic isotope effect requires a transition state having sufficient bond order at N9 to suppress the isotope effect. The C1′–N9 glycosidic bond order could not be increased beyond 0.32 since this caused a decrease in the calculated 1′-^{3}H and ^{14}C kinetic isotope effects below the experimental values. The alternative was to protonate N7, which has the effect of increasing bond order at N9 due to resonance. A proton is required chemically in the reaction mechanism and may serve as an acid catalyst to destabilize the glycosidic linkage by introduction of a positive charge. The combined solvent and substrate kinetic isotope effects make it likely that in the transition state a proton donor has completed or nearly completed transfer of a proton to N7. The sum of bond order in the hypoxanthine ring is greater in the transition state than in the reactant state, requiring the presence of a partial positive charge in the ring at the transition state.

Kinetic Isotope Effects at 5′- and 4′-^{3}H. The large isotope effect for the 5′-^{3}H of inosine was surprising, being four bonds removed from the site of bond breaking and formation. Indeed, the AMP nucleosidases show 5′-^{3}H kinetic isotope effects near unity (Mentch et al., 1987; Parkin et al., 1991b), consistent with similar structures for the reactant and transition states at the 5′-carbon of AMP. In contrast, the nucleoside hydrolase transition state differs substantially from those found for the AMP nucleosidases. This difference clearly indicates an enzyme-induced distortion at the 5′-carbon in the transition state.

Since the 5′-^{3}H isotope effect for nucleoside hydrolase is normal (i.e., >1.0), the C5′–H5′ bond experiences a net loosening in the transition state relative to inosine in solution. This could be realized by decreasing the C5′–H5′ bond order or by placing H5′ in a less crowded environment in the transition state. BEBOVIB calculations reveal that the 5′-^{3}H isotope effect may arise from changes in any of the three angle-bending modes involving H5′ or from decreases in the bond orders of any of the bonds within two atoms of H5′. Factors which could effect this change in bond order include a long-range electronic interaction of H5′ with the oxocarbonium ion, hydrogen bonding of the O5′ hydroxylic hydrogen to either the enzyme or the substrate itself, or a flattening of the sp^3 hybridization at C5′. AMPAC modeling indicates that the C4′–O4′ bond is lengthened due to the adjacent oxocarbonium ion. Decrease in the C4′–O4′ bond order arises from a resonance contributor of the oxocarbonium ion in which C4′–O4′ bond decrease contributes the electron pair to oxygen with a developing positive charge on C4′. An aligned C5′–H5′ bond could hyperconjugate with the developing positive charge at C4′. Further theoretical and experimental observations are necessary to more fully predict the isotope effects which arise from these interactions.

AMPAC calculations on ethanol suggest that a hydrogen bond from the 5′-hydroxyl to an acceptor would cause an increase in the H5′–C5′ bond length and a decrease in the length of the C5′–O5′ bond. These two changes would result in small normal and inverse isotope effects, respectively, but they effectively cancel one another. Thus, simple, in-line hydrogen bonding is unlikely. Alternatively, the 5′-hydroxyl could serve as a lever through which the substrate is held in a reactive conformation to result in a flattening or distortion of the hydroxymethyl group. BEBOVIB calculations indicate that a 3° change in bond angles at the hydroxymethyl group in the directions shown in Figure 5 would result in a 5′-^{3}H isotope effect of 1.05. An interaction with the hydroxymethyl group sufficient to result in its distortion is also likely to stiffen the O5′–C5′–H5′ bending mode. Increase in the angle-bending force constant by 10% resulted in an inverse isotope effect of 0.96, demonstrating that simple "anchoring" of the hydroxymethyl group cannot be the sole source of the 5′-^{3}H isotope effect. Changes in force constants could nonetheless play a role in contributing to the *observed* isotope effect by acting to reduce the magnitude of a normal isotope effect which arises due to flattening of the hydroxymethyl group. Parkin et al. (1991a) have shown that 5′-deoxynucleosides are not substrates for nucleoside hydrolase yet they are inhibitors with K_i values approximately double the K_m for the corresponding substrates. These results, together with the kinetic isotope effects, implicate a transition-state function for the 5′-hydroxyl. A hydrogen bond from the protein to the 5′-hydroxyl could serve as a lever which orients the substrate in a reactive conformation, distorts the geometry at C5′, and gives the observed isotope effect. Until the validity of long-range electronic interaction between H5′ and the oxocarbonium can be evaluated, the preferred interpretation of the 5′-^{3}H isotope effect is from binding distortion which occurs in the transition state.

The inverse 4′-^{3}H kinetic isotope effect is consistent with an increased bond order at C4′–H4′ in the transition state or a more restricted environment. BEBOVIB modeling indicated that the isotope effect is sensitive to changes in bond stretches and/or bond angle bends in which H4′ is involved. The sp^2 hybridization at C1′ in the transition state results in changes in the bond lengths of the ribose ring atoms, which in turn perturb the angle-bending modes involving H4′. Another contribution to the observed 4′-^{3}H kinetic isotope effect might be a change of the H4′–C4′–O4′ force constant, due to the adjacent oxocarbonium ion. The small magnitude of this

isotope effect and the several possible sources for it make the assignment of its origin uncertain. However, it is clear that long-range kinetic isotope effects are due to unique conformations and interactions which occur in the transition state.

Enzyme Contributions to Transition-State Stabilization. Nucleoside hydrolase contains two active site anions having overlapping pK's near 6.1 (Parkin et al., 1991a). The two groups are manifested in the V_{max} and V_{max}/K_m profiles but not in the K_m profile and are therefore involved in transition-state interactions but not in substrate binding. The transition state deduced from isotope effects contains two regions of positive charge, one corresponding to the oxocarbonium ion and the other corresponding to the excess bond order in the departing hypoxanthine ring. It is possible that one or both of the anions (perhaps carboxylates) in the active site are responsible for transition-state stabilization through interaction with the positively charged regions of the transition state. A common feature proposed for glycosidase catalysis is the carboxylate stabilization of carbocationic transition states (Sinnott, 1990; Kajimoto et al., 1991).

In addition to these interactions, one additional group must be involved in the protonation at N7. Since this donor must be protonated to be functional, the pK_a value for this group may be outside the range of the pK_a profile experiment (pH 5–9.5; Parkin et al., 1991a). Another group would be expected to accept the proton from H_2O to form the attacking hydroxyl. It is possible that one of the groups with a pK value of 6.1 could be a proton acceptor for the enzyme-activated nucleophile. Structural or additional pH-reactivity studies will be required to resolve these enzymic contributions to the transition-state structure.

The large isotope effects observed for the 2′-^{3}H and the remote 5′-^{3}H kinetic isotope effects argue for a transition state held in a reactive conformation by the enzyme. The importance of the 2′-, 3′-, and 5′-hydroxyls for catalysis (Parkin et al., 1991a) suggests that the transition-state structure is oriented in part via hydrogen bonds to all hydroxyls of the ribose ring. The family of kinetic isotope effects reported here and the associated transition-state analysis indicate that it may be possible to obtain complete conformational analysis of a transition state using an extension of these methods. Multiple remote isotope effects demonstrate the potential to allow for a precise definition of the ribose ring conformation in the transition state.

Transition-State Inhibitor Design. The combination of multiple heavy atom kinetic isotope effects and transition-state analysis provides a new approach toward inhibitor design. Transition states determined by this approach provide a snapshot of transition-state structure unavailable by X-ray crystallographic, NMR, or other static spectroscopic techniques. Incorporation of key transition-state features in a stable, ground-state molecule should provide specific enzyme inhibitors with high affinities for the target enzyme. The ideal inhibitor must match the transition state geometrically, electronically, and for H-bond ligands. The nucleoside hydrolase transition state described here suggests inhibitors having the following properties. A C-nucleoside linkage would serve to mimic a lengthened glycosidic linkage and confer stability against hydrolysis. The oxocarbonium ion and aglycon positive charge should be represented by incorporation of positive charges into the inhibitor. The 9-^{15}N isotope effect indicates protonation at N7 in the transition state. A basic group or H-bond acceptor in the appropriate position of the inhibitor should enjoy the same interaction. Hydroxyl groups at the 2′-, 3′-, and 5′-positions of the ribose ring are also requisite functional groups, on the basis of the isotope effects and steady-state kinetic properties of the 2′- and 5′-deoxy-compounds (Parkin et al., 1991a). An analogue incorporating these features would be expected to be an exceptional inhibitor on the basis of the unique knowledge of transition-state structure available from kinetic isotope effects and transition-state analysis.

Conclusion

The transition state for nucleoside hydrolase can be described within narrow limits as a structure with well-defined bond lengths and conformational properties. The transition state has substantial oxocarbonium ion character, a protonated leaving group, the glycosidic linkage largely cleaved, and an enzyme-directed attacking O nucleophile just within bonding distance but having low bond order to its target carbon. The ribose portion of the nucleoside is held in a reactive conformation via interactions with its hydroxyl groups. The observation of kinetic isotope effects remote from the site of bond breaking enables extension of the use of enzyme kinetic isotope effects to report on binding and/or conformational phenomena which are unique to enzymic transition states. These results indicate that it is now possible to deduce novel transition-state conformations by a combination of kinetic isotope effects and BEBOVIB analysis. This information provides a glimpse at the transition state not possible using only crystallographic or other spectroscopic approaches which examine ground-state populations. Transition-state structure can be applied to the design of transition-state analogue inhibitors which mimic electronic, geometric, and hydrogen-bonding transition-state features.

References

Cleland, W. W. (1977) *Adv. Enzymol. Relat. Areas Mol. Biol. 45*, 273–387.

Dewar, M. J. S., Zoebisch, E. F., Healy, J. J. P., & Stewart, J. (1985) *J. Am. Chem. Soc. 107*, 3902–3909.

Fersht, A. R. (1977) *Enzyme Structure and Mechanism*, W. H. Freeman & Co., San Francisco.

Hammes, G. G., & Schimmel, P. R. (1970) *The Enzymes 2*, 67–114.

Hammond, G. S. (1955) *J. Am. Chem. Soc. 77*, 334–338.

Johnson, R. W., Marschner, T. M., & Oppenheimer, N. J. (1988) *J. Am. Chem. Soc. 110*, 2257–2263.

Kajimoto, T., Liu, K. K.-C., Pederson, R. L., Zhong, Z., Ichikawa, Y., Porco, J. A., & Wong, C.-H. (1991) *J. Am. Chem. Soc. 113*, 6187–6196.

Kinoshita, Y., Ruble, J. R., & Jeffrey, G. A. (1981) *Carbohydr. Res. 92*, 1–7.

Markham, G. D., Parkin, D. W., Mentch, F., & Schramm, V. L. (1987) *J. Biol. Chem. 262*, 5609–5615.

Mentch, F., Parkin, D. W., & Schramm, V. L. (1987) *Biochemistry 26*, 921–930.

Munns, A. R. I. & Tollin, P. (1970) *Acta Crystallogr., Sect. B 26*, 1101–1113.

Parkin, D. W., & Schramm, V. L. (1984) *J. Biol. Chem. 259*, 9411–9417.

Parkin, D. W., & Schramm, V. L. (1987) *Biochemistry 26*, 913–920.

Parkin, D. W., Leung, H. B., & Schramm, V. L. (1984) *J. Biol. Chem. 259*, 9411–9417.

Parkin, D. W., Horenstein, B. A., Abdulah, D. R., Estupiñán, B., & Schramm, V. L. (1991a) *J. Biol. Chem.* (in press).

Parkin, D. W., Mentch, F., Banks, G. A., Horenstein, B. A., & Schramm, V. L. (1991b) *Biochemistry 30*, 4586–4594.

Romero, R., Stein, R., Bull, H. G., & Cordes, E. H. (1978) *J. Am. Chem. Soc. 100*, 7620–7624.

Schuber, F., Travo, P., & Pascal, M. (1976) *Eur. J. Biochem. 69*, 593-602.
Sims, L. B., & Fry, A. (1974) Special Publication No. 1, University of Arkansas, Fayetteville, AR.
Sims, L. B., & Lewis, D. E. (1984) *Isot. Org. Chem. 6*, 161-259.
Sims, L. B., Burton, G. W., & Lewis, D. E. (1977) Quantum Chemistry Program Exchange, No. 337, Indiana University, Bloomington, IN.
Sinnott, M. L. (1990) *Chem. Rev. 90*, 1171-1202.
Sunko, D. E., Szele, I., & Hehre, W. J. (1977) *J. Am. Chem. Soc. 99*, 5000-5002.
Swain, G. G., Stivers, E. C., Reuner, J. F., & Schadd, L. J. (1958) *J. Am. Chem. Soc. 80*, 5885-5893.
Wilson, E. B., Decius, J. C., & Cross, P. C. (1955) *Molecular Vibrations*, McGraw-Hill Book Co., Inc., New York.

A Protease Activity Associated with Acetylcholinesterase Releases the Membrane-Bound Form of the Amyloid Protein Precursor of Alzheimer's Disease†

David H. Small,*,‡ Robert D. Moir,‡ Stephanie J. Fuller,‡ Samantha Michaelson,‡ Ashley I. Bush,‡ Qiao-Xin Li,‡ Elizabeth Milward,‡ Caroline Hilbich,§ Andreas Weidemann,§ Konrad Beyreuther,§ and Colin L. Masters‡

Department of Pathology, The University of Melbourne, and The Mental Health Research Institute of Victoria, Parkville, Victoria 3052, Australia, and Centre for Molecular Biology, University of Heidelberg, Heidelberg, Federal Republic of Germany

Received March 5, 1991; Revised Manuscript Received August 5, 1991

ABSTRACT: Amyloid deposits in the brains of patients with Alzheimer's disease (AD) contain a protein (βA4) which is abnormally cleaved from a larger transmembrane precursor protein (APP). APP is believed to be normally released from membranes by the action of a protease referred to as APP secretase. Amyloid deposits have also been shown to contain the enzyme acetylcholinesterase (AChE). In this study, a protease activity associated with AChE was found to possess APP secretase activity, stimulating the relase of a soluble 100K form of APP from HeLa cells transfected with an APP cDNA. The AChE-associated protease was strongly and specifically inhibited by soluble APP (10 nM) isolated from human brain. The AChE-associated protease cleaved a synthetic βA4 peptide at the predicted cleavage site. As AChE is decreased in AD, a deficiency of its associated protease might explain why APP is abnormally processed in AD.

Alzheimer's disease (AD) is characterized by deposition of amyloid in the intracellular and extracellular compartments of the cerebral cortex. The extracellular amyloid consists of a protein (βA4) of 4000 relative molecular mass (M_r = 4K). βA4 comprises part of the membrane-spanning and extracellular domains of a much larger precursor protein (APP) of 110-130K, which has features of an integral transmembrane cell surface receptor (Kang et al., 1987). At least three APP isoforms, produced by alternative mRNA splicing, contain an extra 56-residue domain similar to Kunitz type protease inhibitors (KPI) (Kitaguchi et al., 1988; Ponte et al., 1988; Tanzi et al., 1988).

Proteolysis of APP results in the secretion of a 100-110K ectodomain, the KPI-containing forms of which are identical to protease nexin II (Oltersdorf et al., 1989; Van Nostrand et al., 1989), a protease inhibitor that may be involved in neurotrophic mechanisms. Recent studies suggest that the normal cleavage of APP occurs at or near a lysine residue within the βA4 sequence (Esch et al., 1990). Cleavage of this site would prevent formation of the amyloidogenic βA4 fragment. The protease which cleaves at this site ("APP secretase") has not been identified, but a deficiency in this enzyme might lead to abnormal processing of APP and production of amyloidogenic βA4.

The cholinergic system is vulnerable in AD, resulting in a reduction in the cholinergic enzymes acetylcholinesterase (AChE) (Davies & Maloney, 1976; Davies, 1979; Fishman et al., 1986; Hammond & Brimijoin, 1988) and choline acetyltransferase (Bowen et al., 1976; Davies & Maloney, 1976). Despite the substantial depletion of AChE in the AD brain, the enzyme accumulates within both amyloid plaques (Friede, 1965; Struble et al., 1982) and tangles (Mesulam & Moran, 1987; Carson et al., 1991). An AChE-associated protease (AChE-AP) with both trypsin-like and carboxypeptidase activities is recovered with AChE purified by affinity chromatography from tissues rich in AChE such as fetal bovine serum or eel electroplax organ (Small et al., 1987; Small, 1988). The trypsin-like activity of AChE-AP is associated with a 25K protein which may bind to AChE or may be a fragment of AChE produced through proteolysis of an AChE catalytic subunit (Small & Simpson, 1988; Small, 1990).

The substrate for the AChE-AP has not been identified. In this paper, we provide evidence that the AChE-AP may possess an "APP secretase" function, cleaving APP from the cell membrane.

Materials and Methods

Materials. Purified human brain APP was prepared from a soluble extract of post-mortem human brain grey matter by procedures involving heparin-Sepharose, ion-exchange, and dye-ligand chromatography (Moir et al., in preparation). Enzyme inhibitors (aprotinin, leupeptin, soybean trypsin inhibitor, and BW284C51) and crude eel AChE (type V-S) were

† This work was supported by grants from the National Health and Medical Research Council of Australia, the Aluminum Development Corp. of Australia, and the Victorian Health Promotion Foundation. K.B. is supported by the Deutsche Forschungsgemeinschaft and the Bundesministerium für Forschung und Technologie.

* Address correspondence to this author at the Department of Pathology, The University of Melbourne, Parkville, Victoria 3052, Australia.
‡ The University of Melbourne and The Mental Health Research Institute of Victoria.
§ University of Heidelberg.

0006-2960/91/0430-10795$02.50/0